Published in final edited form as:

ACS Chem Biol. 2016 January 15; 11(1): 132–138. doi:10.1021/acschembio.5b00758.

Self-Assembling NanoLuc Luciferase Fragments as Probes for Protein Aggregation in Living Cells

Jia Zhao, **Travis J. Nelson**, **Quyen Vu**, **Tiffany Truong**, and **Cliff I. Stains**

Department of Chemistry, University of Nebraska—Lincoln, Lincoln, Nebraska 68588, United States

Cliff I. Stains: cstains2@unl.edu

Abstract

Given the clear role of protein aggregation in human disease, there is a critical need for assays capable of quantifying protein aggregation in living systems. We hypothesized that the inherently low background and biocompatibility of luminescence signal readouts could provide a potential solution to this problem. Herein, we describe a set of self-assembling NanoLuc luciferase (Nluc) fragments that produce a tunable luminescence readout that is dependent upon the solubility of a target protein fused to the N-terminal Nluc fragment. To demonstrate this approach, we employed this assay in bacteria to assess mutations known to disrupt amyloid-beta (Aβ) aggregation as well as disease-relevant mutations associated with familial Alzheimer's diseases. The luminescence signal from these experiments correlates with the reported aggregation potential of these Aβ mutants and reinforces the increased aggregation potential of disease-relevant mutations in A$\beta_{1–42}$. To further demonstrate the utility of this approach, we show that the effect of small molecule inhibitors on Aβ aggregation can be monitored using this system. In addition, we demonstrate that aggregation assays can be ported into mammalian cells. Taken together, these results indicate that this platform could be used to rapidly screen for mutations that influence protein aggregation as well as inhibitors of protein aggregation. This method offers a novel, genetically encodable luminescence readout of protein aggregation in living cells.

Graphical abstract

Correspondence to: Cliff I. Stains, cstains2@unl.edu.

Supporting Information: The Supporting Information is available free of charge on the ACS Publications website at DOI: 10.1021/acschem-bio.5b00758.

Notes: The authors declare no competing financial interest.

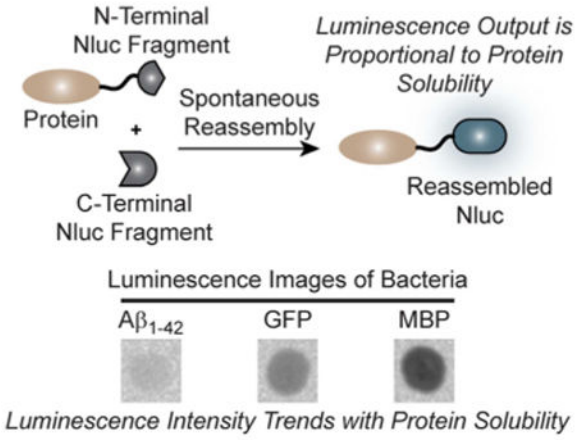

Protein aggregation is now recognized as a defining component of numerous human disease states including Alzheimer's (Aβ), Huntington's (huntingtin), and Parkinson's (α-synuclein) disease as well as type 2 diabetes (amylin).[1] As a consequence, there is significant interest in understanding the mechanisms of protein aggregation[2–4] as well as identifying compounds capable of modulating this process.[5–7] However, efforts to develop such compounds have been hindered by the paucity of assays capable of sensitively reporting on protein aggregation in living cells in a high-throughput format. One approach to this problem has been to monitor the influence of proteins fused to the N-terminus of reporters such as GFP, β-galactosidase, or chloramphenicol acetyltransferase.[8–10] Indeed, the Hecht laboratory has employed Aβ-GFP fusions to identify novel inhibitors of Aβ aggregation.[6] Although powerful, these methodologies are limited by the inherent detection limits of colorimetric- and fluorescence-based assays as well as potential false positives due to autofluorescent compounds. Consequently, we set out to investigate luminescence as an alternative detection modality since luminescence-based assays afford relatively high sensitivity and lower background compared to colorimetric- and fluorescence-based approaches. In addition, luminescence-based assays are commonly used for imaging in living organisms,[11,12] allowing for the long-term possibility of monitoring compound efficacy in animal models of disease.

In order to generate a genetically encodable sensor of protein aggregation, we turned our attention to self-assembling split-protein reporter systems. Interestingly, compared to conditional split-protein reassembly systems which have been extensively employed to detect protein–protein interactions in living systems,[13–18] self-assembling split-protein systems have been relatively underexplored. One notable exception is the self-assembling GFP fragments described by the Waldo laboratory.[19] Using this system, one can monitor the solubility of a protein by fusion to a self-assembling GFP fragment. Expression of this fusion protein in the presence of the complementary fragment results in recovery of GFP fluorescence that is proportional to the solubility of the appended protein. This approach has been used to readily identify solubilizing mutations for a variety of proteins.[20,21] However, this methodology is limited by the lag time of GFP chromophore formation after reassembly, potentially hindering real-time analysis. One alternative approach is to utilize luciferase enzymes to monitor protein aggregation in living cells.[22] A promising strategy in this area is

to leverage the conditional reassembly of split-luciferase fragments to detect protein aggregation.[23] Although numerous conditional split-luciferase systems have been described,[24–27] self-assembling luciferase platforms have received relatively little attention.[28,29] We hypothesized that a thermostable luciferase may provide an appropriate scaffold for the discovery of self-assembling luciferase fragments. Nluc[30,31] is a recently described, engineered luciferase capable of producing a robust luminescence signal using either coelenterazine or furimazine as a substrate. The Nluc scaffold displays enhanced thermostability relative to firefly luciferase and is not sensitive to unfolding/refolding cycles. Herein, we present the discovery of self-assembling Nluc fragments capable of producing a luminescence signal within seconds upon mixing. We further demonstrate the utility of these fragments by monitoring protein solubility in living cells, as well as the effect of small molecules on protein aggregation using a straightforward assay format (Figure 1).

Results and Discussion

In the absence of a crystal structure of Nluc, we chose to employ computational modeling in order to identify potential solvent exposed loops as sites for fragmentation in Nluc.[32,33] This analysis yielded five possible fragmentation sites (Figure S1 and Table S1). In order to assess the ability of these fragments to self-assemble, we cloned each fragment into separate compatible vectors for expression in bacteria. Cotransformation and expression of these fragments in bacteria yielded four hits capable of self-assembly as judged by luminescence imaging of bacteria (Figure 2a). Separate expression of each of these fragments yielded no observable background luminescence in cells (Figure 2a). Building upon these promising results, we next investigated the magnitude of the luminescence signal obtained from each self-assembling pair by normalizing bacterial cultures based on cell density and monitoring luminescence of cell suspensions on a plate reader. These data demonstrated that the maximal luminescence signal was generated by the Nluc fragment combination corresponding to residues 1–65 (N65) and 66–171 (66C; Figure 2b). Identical results were obtained when Nluc fragments were expressed separately and the resulting lysates were mixed (Figure S2). The luminescence signal from these assays did not increase after mixing (Figure S3), indicating that reassembly occurs within seconds of mixing the protein components. These data convincingly demonstrate that a direct interaction between Nluc fragments after translation is responsible for the observed increase in luminescence. In addition, no detectable luminescence was observed in these lysates prior to mixing with the complementary fragment (Figure S2). Taken together, these results suggest that Nluc provides a robust structure for the identification of self-assembling protein fragments capable of rapid association to produce a luminescent complex in living cells.

To further assess reassembly in this system, we separately purified the N65 and 66C fragments using immobilized metal ion affinity chromatography. Although the yields of 66C were relatively low compared to N65 (0.07 mg versus 0.8 mg per liter of culture, respectively), we were able to obtain sufficient quantities of protein for *in vitro* analysis (Figure 3a). Interestingly, we observed a weak luminescence signal from 66C alone at 50 nM (Figure 3b). However, the addition of excess N65 led to a robust 10-fold increase in luminescence that was not accounted for by the sum of the luminescence of either fragment alone (Figure 3b). These data suggest that the concentration of soluble 66C within living

cells is below the detection limit of the luminescence assay, providing a turn-on luminescence signal that is proportional to the concentration of N65 with essentially undetectable background (Figure 2). This hypothesis is further supported by control experiments, which indicate that coexpression of the N65 and 66C fragments leads to an increase in the total expression level of 66C (Figure S4). This effect is presumably due to the increased solubility of the reassembled enzyme. Moreover, the poor solubility and expression level of 66C alone is likely responsible for the low yield of this fragment during purification. Reassembled Nluc could be detected using either coelenterazine or the optimized substrate furimazine (Figure S5). Titration of 66C with increasing amounts of N65 indicated that the luminescence response from these fragments was linear over 3 orders of magnitude under these assay conditions, clearly demonstrating the ability to correlate the luminescence signal to protein concentration (Figure 3c). Comparison of the luminescence intensity of reassembled N65 and 66C to a calibration curve constructed using known concentrations of full-length Nluc (Figure S6) indicated that reassembly efficiency was ~0.1% using 10 μM N65 and 10 μM 66C. This level of efficiency is comparable to that observed in other split-protein systems.[34] Monitoring luminescence response over time after mixing purified proteins indicated that reassembly had occurred within the time used for assay preparation (seconds time scale, see Figure S7). Similar results were obtained when N65 and 66C fragments were mixed and luminescence was measured by the addition of coelenterazine at different time points up to 2 h (Figure 3d). Together, these results indicate that reassembly occurs rapidly upon mixing of the complementary fragments.

Building upon these results, we reasoned that modulation of the solubility of N65 in cells could directly impact the extent of Nluc reassembly and serve as a sensitive readout of the solubility of proteins fused to N65 (Figure 1). As a first step toward this goal, we determined whether the relative trends in solubility of the well-characterized proteins GFP,[35] maltose binding protein (MBP),[36] and Aβ_{1-42}[4,6] were perturbed in this assay system. We fused each of these proteins to the N-terminus of N65; yielding GFP-N65, MBP-N65, and Aβ_{1-42}-N65 (Table S2). Coexpression of these three N65 fusions together with 66C resulted in a dramatic modulation of luminescence signal in intact cells that trended with the relative solubility of these proteins (Figure 4). Moreover, Western blotting analysis of soluble N65 fusions directly correlated to the observed luminescence in this system (Figure 4). Importantly, fusion of MBP to the N-terminus of 66C resulted in poor luminescence recovery, possibly due to inhibition of Nluc reassembly (Figure S8).

Building upon these results, we then asked whether this system could report on the effect of point mutations that are known to decrease the aggregation potential of Aβ_{1-42}.[4] Accordingly, we chose the GM18, GM33, and GM6 mutants described by the Hecht laboratory, which display increased lag times for aggregation compared to wild-type protein. Importantly, using a GFP solubility assay, these point mutants have been shown to display 33% (GM18), 45% (GM33), and 100% (GM6) fluorescence relative to the wild-type Aβ_{1-42} (5% fluorescence recovery).[4] Fusion of these Aβ_{1-42} mutants to the N-terminus of N65 (Table S2) resulted in a predictable alteration in luminescence signal within living cells that correlated with the published GFP-based assay data (Figure 5a). This change in luminescence intensity was proportional to the amount of soluble protein and was not due to changes in overall protein expression levels (Figure S9). To further assess the utility of this

system we probed to affect disease-related mutations in A$\beta_{1–42}$ on luminescence signal output in living bacteria. Specifically, we chose the D23N (Iowa)[37] and E22G (Arctic)[38] mutations, which were identified through sequencing of individuals in families with early onset Alzheimer's. Comparison of recovered luminescence in cells expressing N-terminal fusions of these mutations to N65 yielded 23 and 54% decreases in luminescence relative to wild-type A$\beta_{1–42}$, for the D23N and E22G mutants respectively (Figure 5b). These results are in agreement with previous work that indicates an increased aggregation potential for these mutants compared to wild-type A$\beta_{1–42}$,[38–41] indicating that the split-Nluc fragments can be used to assess the aggregation potential of disease-relevant mutations. Although it is possible that highly soluble N65 fusions could exhaust the cellular pool of 66C leading to a nonlinear response from this assay system, we do not observe this phenomenon using the panel of fusion proteins described in this work (Figures 4, 5, and S9). Furthermore, Western blot analysis can be used as a secondary assay to validate results from the luminescence assay. Taken together, these data demonstrate the ability of this platform to identify mutations that alter A$\beta_{1–42}$ aggregation potential as well as probe the influence of disease-relevant mutations on aggregation.

In a broader context, these results show that this assay platform could be utilized to screen for inhibitors of protein aggregation. As a proof-of-principle, we asked whether we could monitor the inhibition of A$\beta_{1–42}$ fibrillization using o-vanillin.[42] First, we generated lysates of cells expressing either A$\beta_{1–42}$-N65 or 66C and assessed whether we could monitor aggregation of A$\beta_{1–42}$ over time by addition of 66C (Figure 6a). Indeed, we observed a time-dependent decrease in luminescence signal, indicating that this approach could be used to monitor the kinetics of A$\beta_{1–42}$ aggregation in a similar format to traditional thioflavin T assays. Although it should be noted that in this context amyloid species may already be present and provide nucleation sites for further aggregation. We next asked whether the effect of o-vanillin could be assessed using this system. Indeed, addition of o-vanillin to A$\beta_{1–42}$-N65 lysates resulted in a 19% increase in luminescence (Figure 6b). This inhibitory effect is similar to that observed previously for o-vanillin.[42] In the long term, we expect that this assay platform could be used to identify noncytotoxic, membrane permeable small molecule inhibitors of A$\beta_{1–42}$ aggregation.

One potential utility of this genetically encodable protein aggregation assay would be the ability to assess protein aggregation in mammalian cells. In order to first determine whether reassembly of Nluc in mammalian cells could be monitored, we transfected NIH-3T3 cells with vectors expressing N65 or 66C and compared recovered luminescence to cells that had been cotransfected with N65 and 66C. Live cell luminescence measurements using furimazine as a substrate clearly indicated that luminescence was only observed in cells expressing both Nluc fragments, while expression of N65 or 66C alone produced background levels of luminescence (Figure 7a). Next, we asked whether the relative differences in the luminescence of A$\beta_{1–42}$, GM18, or GM6 fusions to N65 (Figure 5a) could be monitored in mammalian cells. As expected, we observed clear increases in the luminescence signal obtained from the GM18 and GM6 fusions that correlated with the results obtained in bacteria (Figure 7b). Taken together, these data indicate the ability to leverage this methodology to identify mutations as well as small molecules in bacterial

systems amenable to high-throughput screening and subsequently port these assays into more relevant mammalian cell systems.

In conclusion, we have described several self-assembling Nluc fragments based on dissection at predicted solvent exposed loops. Reassembly and resulting luminescence output of the fragments termed N65 and 66C can be modulated by the solubility of proteins fused to N65. This property allows for the sensitive detection of protein solubility in a straightforward, high-throughput assay format in living cells. The ability to detect disease-relevant mutations that influence the aggregation potential of proteins indicates that this assay platform could find utility in high-throughput screening of protein aggregation inhibitors. As a proof-of-concept, we have demonstrated the ability to assess the influence of small molecules on Aβ_{1-42} aggregation. In addition, we have shown that assays can be ported into mammalian cell systems. Our laboratory is currently investigating the fundamental determinants of aggregation in several disease-relevant proteins as well as screening for inhibitors of protein aggregation. We are also investigating the ability to utilize these fragments to detect protein localization in mammalian cell systems[43,44] as well as employing mutagenesis to afford fragments capable of conditional reassembly that could be used to probe protein–protein interactions in living systems.

Methods

General Methods

Proteins isolated from immobilized metal ion chromatography were further purified by FPLC on an AKTAprime-Plus (GE Healthcare) with a HiLoad 16/600 Superdex 75pg column (GE Healthcare). Protein absorbance was monitored at 280 nm.

Protein concentrations were determined using a BioMate 3S UV–visible spectrophotometer (Thermo Scientific).

Luminescence images were captured on a Gel Doc XR+ system. Luminescence intensities were quantified using a SynergyH1 hybrid reader (BioTek). Plates were either Corning 96-well assay plates (3359) [white, half area, round-bottom, 120 μL reaction volume] or Corning 384-well assay plates (3824) [white, low volume, flat bottom, 40 μL reaction volume]. Luminescence readings in living bacteria were obtained 30 min after substrate addition; all other luminescence readings were acquired immediately after substrate addition, unless indicated otherwise. Relative luminescence data were obtained by dividing raw luminescence readings by the largest luminescence value obtained in each experiment.

Recipes for buffers and stock solutions can be found in the Supporting Information. TB medium is terrific broth.

Identification and Cloning of Nluc Fragments

Details can be found in the Supporting Information.

Luminescence Imaging of Bacteria

BL21-Gold (DE3) competent cells (Stratagene) were singly transformed with either the pET-45b N-terminal Nluc fragment plasmid or the pRSF-1b C-terminal Nluc fragment plasmid. Cultures were grown from single colonies to an OD_{600} = 0.6–0.8 at 37 °C, with shaking at 250 rpm. Cultures were then cooled to 16 °C, and the cells were induced with 0.2 mM IPTG and grown overnight. Cell cultures were normalized to an OD_{600} = 3.0 in 1 mL. Cells were harvested by centrifugation at 700*g* for 10 min at 4 °C and resuspended in 15 μL of 50 μM colenterazine. The reaction mixture was immediately spotted on a nitrocellulose membrane and imaged using a Gel Doc XR+ system.

Luminescence Assays Using Cell Lysates

Cultures were induced as above and normalized to an OD_{600} = 3.0 in 2 mL, and cells were harvested at 17 000*g* for 10 min. Cell samples were lysed using the B-PER Bacterial Protein Extraction Reagent (Life Technologies, 100 μL), following the vendor recommended protocol. Soluble fractions were collected after centrifugation and used in the following assay. For the assay reaction, 48 μL of N-terminal fragment lysate, 48 μL of C-terminal fragment lysate, 99 uL of 2× Nluc assay buffer (see Supporting Information for recipe), and 195 μL of 50 μM colenterazine in 1× Nluc assay buffer were mixed. For control reactions, 48 μL of N- or C-terminal fragment lysate, 48 μL of B-PER, 99 uL of 2× assay buffer, and 195 of μL of 50 μM colenterazine were mixed.

Expression and Purification of N65 and 66C Nluc Fragments

The pET-45b N65 or pRSF-1b 66C plasmids were singly transformed into BL21- Gold (DE3) competent cells (Stratagene) and grown at 37 °C to mid log phase in 1 L of TB media with the appropriate antibiotic. The culture was cooled to 16 °C, and the cells were induced with 0.2 mM IPTG and grown overnight. Cells were harvested by centrifugation at 3220*g* for 30 min at 4 °C, washed with DI water, and frozen at −80 °C. For cell lysis, pellets were thawed and resuspended in 40 mL of 1× PBS containing 1 mg mL^{-1} lysozyme and incubated for 20 min at 4 °C. The cells were then sonicated at 40% amplitude using 1 s on and 1 s off cycles for a total of 45 s. Lysates were clarified by centrifugation at 18 000*g* for 60 min, followed by incubation with HisPur Ni-NTA resin (Thermo Scientific, 500 μL resin per 1L cell culture). Prior to incubation with lysate, the resin was equilibrated with 20 mL of 1× PBS. Lysates were incubated with resin for 1 h under rotation at 4 °C. Ni-NTA resin was then collected and washed with increasing concentrations of imidazole in 1× PBS (100 mL of 10 mM imidazole followed by 100 mL of 50 mM imidazole). Protein was eluted with 5 mL of 500 mM imidazole in 1× PBS. Eluted proteins were further purified via FPLC using 1× PBS as the mobile phase. Fractions containing the desired protein as assessed by SDS-PAGE (N65 molecular weight = 10 289 Da and 66C molecular weight = 13 530 Da) were combined and concentrated using 3.5 kDa MWCO Amicon Ultra-15 centrifugal filters via centrifugation at 3220*g* at 4 °C. Concentrations of N65 were determined by measuring absorbance at 280 nm (N65 molar extinction coefficient = 13 980 M^{-1} cm^{-1}). Concentrations of 66C were estimated from gels by comparison to N65.

Titration of 66C with N65

The 66C fragment (384 nM) was mixed with increasing concentrations of N65 fragment (50 nM, 100 nM, 200 nM, 500 nM, 1 μM, 2.5 μM, 5 μM, 10 μM, 15 μM, and 20 μM) in an assay reaction containing 50 μM coelenterazine and 1× PBS (total volume of the assay was 120 μL).

Cloning of Amyloid-Beta-, GFP-, and MBP-N65 Fusions

Full details can be found in the Supporting Information.

Aβ_{1-42} GM Mutant Protein Solubility Assays

BL21-Gold (DE3) cells were cotransformed with vectors containing the N-terminal fusions of the indicated proteins to N65 as well as a vector expressing 66C (full sequence details can be found in Tables S1 and S2). Single colonies were used to inoculate 8 mL of TB media containing ampicillin and kanamycin. Cultures were grown to an OD_{600} = 0.6–0.8 at 37 °C, 250 rpm. Cultures were then cooled to 16 °C, and the cells were induced with 0.2 mM IPTG and grown overnight. The next morning, cell cultures were normalized to an OD_{600} = 3.0 in 1 mL. Cells were harvested by centrifugation at 700*g* for 10 min at 4 °C and resuspended in 1× Nluc assay buffer (200 μL). An equal volume of cell culture (195 μL) and 50 μM coelenterazine were mixed in order to initiate the luminescence assay.

Disease-Relevant Aβ_{1-42} Mutant Assays

BL21-Gold (DE3) cells were cotransformed with vectors containing the N-terminal fusions of Aβ_{1-42} mutants D23N, E22G, or wild-type Aβ_{1-42} (Table S2) to N65 as well as a vector expressing 66C. Single colonies were used to inoculate 8 mL of TB medium containing ampicillin and kanamycin. Cultures were grown to an OD_{600} = 0.6–0.8 at 37 °C, 250 rpm and were induced with 1 mM IPTG and grown for 3 h. Cell cultures were normalized to an OD_{600} = 3.0 in 1 mL. Cells were harvested by centrifugation at 700*g* for 10 min at 4 °C and resuspended in 1× Nluc assay buffer (200 μL). An equal volume of cell culture (195 μL) and 50 μM coelenterazine were mixed in order to initiate the luminescence assay.

Western Blotting Conditions

Western blotting conditions are provided in the Supporting Information.

Monitoring Inhibition of Aβ_{1-42} Aggregation

BL21-Gold (DE3) cells were singly transformed with a vector expressing Aβ_{1-42}-N65 or 66C. Single colonies were used to inoculate 20 mL of TB media containing ampicillin or kanamycin. Cultures were grown to an OD_{600} = 0.6–0.8 at 37 °C, 250 rpm. Cultures were then cooled to 16 °C, and the cells were induced with 0.2 mM IPTG and grown overnight. The next morning, cell cultures were harvested at 17 000*g* for 10 min. Cell samples were lysed using B-PER (1000 μL), following the vendor recommended protocol. Soluble proteins were collected after centrifugation and used in the following assay. Cell lysate from cells expressing Aβ_{1-42}-N65 (150 μL) were mixed with 50 μL of PBS with or without o-vanillin (10 μM final concentration). Assay reactions were incubated at 37 °C for 3 h. Similarly, assay reactions without o-vanillin were also set up and incubated at 37 °C. After

incubation for the indicated time, the A$\beta_{1–42}$-N65 lysate was mixed with cell lysate containing the 66C Nluc fragment (50 μL) and incubated at RT for 5 min. An equal volume (195 μL) of lysate mixture and 50 μM colenterazine were mixed, and luminescence was measured on a plate reader.

Cloning of Mammalian Cell Expression Constructs

Full details can be found in the Supporting Information.

Mammalian Cell Experiments

NIH-3T3 cells were seeded in 96-well plates in 200 μL of complete growth media (DMEM + 10% FBS + 1% penicillin-streptomycin) and grown overnight at 37 °C with 5% CO_2. The following day, cells were cotransfected with vectors containing N65 and 66C Nluc fragments (see Table S3 for sequences), 100 ng each, using Lipofectamine 3000 Reagent (Invitrogen) according to manufacturer protocols. As a control, NIH-3T3 cells were singly transfected with either N65 or 66C vector, 100 ng. Mock transfections (lipid complexes without DNA) were also conducted. Cells were grown overnight at 37 °C, and after 20 h the medium was aspirated and replaced with growth media without phenol red. Nano-glo substrate (Promega) was added to initiate the luminescence assay according to manufacturer protocols. Luminescence values from untreated cells were used for background subtraction.

Aggregation assays with A$\beta_{1–42}$ mutants (see Table S3 for sequences) were performed as above except that 600 ng of each plasmid was used for transfection.

Supplementary Material

Refer to Web version on PubMed Central for supplementary material.

Acknowledgments

T.J.N. was supported by a Molecular Mechanisms of Disease Fellowship (T32GM107001). We gratefully acknowledge funding from the Department of Chemistry at the University of Nebraska—Lincoln.

References

1. Chiti F, Dobson CM. Protein misfolding, functional amyloid, and human disease. Annu Rev Biochem. 2006; 75:333–366. [PubMed: 16756495]
2. Brister MA, Pandey AK, Bielska AA, Zondlo NJ. OGlcNAcylation and phosphorylation have opposing structural effects in tau: phosphothreonine induces particular conformational order. J Am Chem Soc. 2014; 136:3803–3816. [PubMed: 24559475]
3. Nelson R, Sawaya MR, Balbirnie M, Madsen AO, Riekel C, Grothe R, Eisenberg D. Structure of the cross-beta spine of amyloid-like fibrils. Nature. 2005; 435:773–778. [PubMed: 15944695]
4. Wurth C, Guimard NK, Hecht MH. Mutations that reduce aggregation of the Alzheimer's A beta 42 peptide: an unbiased search for the sequence determinants of A beta amyloido-genesis. J Mol Biol. 2002; 319:1279–1290. [PubMed: 12079364]
5. Stains CI, Mondal K, Ghosh I. Molecules that target beta-amyloid. ChemMedChem. 2007; 2:1674–1692. [PubMed: 17952881]
6. Kim W, Kim Y, Mn J, Kim DJ, Chang YT, Hecht MH. A high-throughput screen for compounds that inhibit aggregation of the Alzheimer's peptide. ACS Chem Biol. 2006; 1:461–469. [PubMed: 17168524]

7. Smith TJ, Stains CI, Meyer SC, Ghosh I. Inhibition of beta-amyloid fibrillization by directed evolution of a beta-sheet presenting miniature protein. J Am Chem Soc. 2006; 128:14456–14457. [PubMed: 17090018]
8. Wigley WC, Stidham RD, Smith NM, Hunt JF, Thomas PJ. Protein solubility and folding monitored in vivo by structural complementation of a genetic marker protein. Nat Biotechnol. 2001; 19:131–136. [PubMed: 11175726]
9. Waldo GS, Standish BM, Berendzen J, Terwilliger TC. Rapid protein-folding assay using green fluorescent protein. Nat Biotechnol. 1999; 17:691–695. [PubMed: 10404163]
10. Maxwell KL, Mittermaier AK, Forman-Kay JD, Davidson AR. A simple in vivo assay for increased protein solubility. Protein Sci. 1999; 8:1908–1911. [PubMed: 10493593]
11. Evans MS, Chaurette JP, Adams ST, Reddy GR, Paley MA, Aronin N, Prescher JA, Miller SC. A synthetic cluciferin improves bioluminescence imaging in live mice. Nat Methods. 2014; 11:393–395. [PubMed: 24509630]
12. Adams ST, Miller SC. Beyond D-luciferin: expanding the scope of bioluminescence imaging in vivo. Curr Opin Chem Biol. 2014; 21:112–120. [PubMed: 25078002]
13. Herbst KJ, Allen MD, Zhang J. Luminescent kinase activity biosensors based on a versatile bimolecular switch. J Am Chem Soc. 2011; 133:5676–5679. [PubMed: 21438554]
14. Kerppola TK. Visualization of molecular interactions using bimolecular fluorescence complementation analysis: characteristics of protein fragment complementation. Chem Soc Rev. 2009; 38:2876–2886. [PubMed: 19771334]
15. Magliery TJ, Wilson CG, Pan W, Mishler D, Ghosh I, Hamilton AD, Regan L. Detecting protein-protein interactions with a green fluorescent protein fragment reassembly trap: scope and mechanism. J Am Chem Soc. 2005; 127:146–157. [PubMed: 15631464]
16. Sarkar M, Magliery TJ. Re-engineering a split-GFP reassembly screen to examine RING-domain interactions between BARD1 and BRCA1 mutants observed in cancer patients. Mol BioSyst. 2008; 4:599–605. [PubMed: 18493658]
17. Tarassov K, Messier V, Landry CR, Radinovic S, Serna Molina MM, Shames I, Malitskaya Y, Vogel J, Bussey H, Michnick SW. An in vivo map of the yeast protein interactome. Science. 2008; 320:1465–1470. [PubMed: 18467557]
18. Jackrel ME, Cortajarena AL, Liu TY, Regan L. Screening libraries to identify proteins with desired binding activities using a split-GFP reassembly assay. ACS Chem Biol. 2010; 5:553–562. [PubMed: 20038141]
19. Cabantous S, Terwilliger TC, Waldo GS. Protein tagging and detection with engineered self-assembling fragments of green fluorescent protein. Nat Biotechnol. 2005; 23:102–107. [PubMed: 15580262]
20. Listwan P, Terwilliger TC, Waldo GS. Automated, high-throughput platform for protein solubility screening using a split-GFP system. J Struct Funct Genomics. 2009; 10:47–55. [PubMed: 19039681]
21. Cabantous S, Waldo GS. In vivo and in vitro protein solubility assays using split GFP. Nat Methods. 2006; 3:845–854. [PubMed: 16990817]
22. Fuentealba RA, Marasa J, Diamond MI, Piwnica-Worms D, Weihl CC. An aggregation sensing reporter identifies leflunomide and teriflunomide as polyglutamine aggregate inhibitors. Hum Mol Genet. 2012; 21:664–680. [PubMed: 22052286]
23. Hashimoto T, Adams KW, Fan ZY, McLean PJ, Hyman BT. Characterization of Oligomer Formation of Amyloid-beta Peptide Using a Split-luciferase Complementation Assay. J Biol Chem. 2011; 286:27081–27091. [PubMed: 21652708]
24. Paulmurugan R, Gambhir SS. Monitoring protein-protein interactions using split synthetic renilla luciferase protein-fragment-assisted complementation. Anal Chem. 2003; 75:1584–1589. [PubMed: 12705589]
25. Paulmurugan R, Umezawa Y, Gambhir SS. Noninvasive imaging of protein-protein interactions in living subjects by using reporter protein complementation and reconstitution strategies. Proc Natl Acad Sci U S A. 2002; 99:15608–15613. [PubMed: 12438689]
26. Luker KE, Smith MCP, Luker GD, Gammon ST, Piwnica-Worms H, Piwnica-Worms DP. Kinetics of regulated protein-protein interactions revealed with firefly luciferase complementation imaging

in cells and living animals. Proc Natl Acad Sci U S A. 2004; 101:12288–12293. [PubMed: 15284440]

27. Remy I, Michnick SW. A highly sensitive protein-protein interaction assay based on Gaussia luciferase. Nat Methods. 2006; 3:977–979. [PubMed: 17099704]
28. Hida N, Awais M, Takeuchi M, Ueno N, Tashiro M, Takagi C, Singh T, Hayashi M, Ohmiya Y, Ozawa T. High-sensitivity real-time imaging of dual protein-protein interactions in living subjects using multicolor luciferases. PLoS One. 2009; 4:e5868. [PubMed: 19536355]
29. Misawa N, Kafi AKM, Hattori M, Miura K, Masuda K, Ozawa T. Rapid and high-sensitivity cell-based assays of protein-protein interactions using split click beetle luciferase complementation: an approach to the study of G-protein-coupled receptors. Anal Chem. 2010; 82:2552–2560. [PubMed: 20180537]
30. Hall MP, Unch J, Binkowski BF, Valley MP, Butler BL, Wood MG, Otto P, Zimmerman K, Vidugiris G, Machleidt T, Robers MB, Benink HA, Eggers CT, Slater MR, Meisenheimer PL, Klaubert DH, Fan F, Encell LP, Wood KV. Engineered luciferase reporter from a deep sea shrimp utilizing a novel imidazopyrazinone substrate. ACS Chem Biol. 2012; 7:1848–1857. [PubMed: 22894855]
31. Machleidt T, Woodroofe CC, Schwinn MK, Mendez J, Robers MB, Zimmerman K, Otto P, Daniels DL, Kirkland TA, Wood KV. NanoBRET—a novel BRET platform for the analysis of protein-protein interactions. ACS Chem Biol. 2015; 10:1797–1804. [PubMed: 26006698]
32. Jones DT. Protein secondary structure prediction based on position-specific scoring matrices. J Mol Biol. 1999; 292:195–202. [PubMed: 10493868]
33. Kyte J, Doolittle RF. A Simple Method for Displaying the Hydropathic Character of a Protein. J Mol Biol. 1982; 157:105–132. [PubMed: 7108955]
34. Stains CI, Porter JR, Ooi AT, Segal DJ, Ghosh I. DNA sequence-enabled reassembly of the green fluorescent protein. J Am Chem Soc. 2005; 127:10782–10783. [PubMed: 16076155]
35. Orm M, Cubitt AB, Kallio K, Gross LA, Tsien RY, Remington SJ. Crystal structure of the Aequorea victoria green fluorescent protein. Science. 1996; 273:1392–1395. [PubMed: 8703075]
36. Fox JD, Waugh DS. Maltose-binding protein as a solubility enhancer. Methods Mol Biol. 2003; 205:99–117. [PubMed: 12491882]
37. Grabowski TJ, Cho HS, Vonsattel JPG, Rebeck GW, Greenberg SM. Novel amyloid precursor protein mutation in an Iowa family with dementia and severe cerebral amyloid angiopathy. Ann Neurol. 2001; 49:697–705. [PubMed: 11409420]
38. Nilsberth C, Westlind-Danielsson A, Eckman CB, Condron MM, Axelman K, Forsell C, Stenh C, Luthman J, Teplow DB, Younkin SG, Naslund J, Lannfelt L. The ‘Arctic’ APP mutation (E693G) causes Alzheimer's disease by enhanced A beta protofibril formation. Nat Neurosci. 2001; 4:887–893. [PubMed: 11528419]
39. Chiti F, Stefani M, Taddei N, Ramponi G, Dobson CM. Rationalization of the effects of mutations on peptide and protein aggregation rates. Nature. 2003; 424:805–808. [PubMed: 12917692]
40. Van Nostrand WE, Melchor JP, Cho HS, Greenberg SM, Rebeck GW. Pathogenic effects of D23N Iowa mutant amyloid beta-protein. J Biol Chem. 2001; 276:32860–32866. [PubMed: 11441013]
41. Hori Y, Hashimoto T, Wakutani Y, Urakami K, Nakashima K, Condron MM, Tsubuki S, Saido TC, Teplow DB, Iwatsubo T. The Tottori (D7N) and English (H6R) familial Alzheimer disease mutations accelerate A beta fibril formation without increasing protofibril formation. J Biol Chem. 2007; 282:4916–4923. [PubMed: 17170111]
42. Necula M, Kayed R, Milton S, Glabe CG. Small molecule inhibitors of aggregation indicate that amyloid beta oligomerization and fibrillization pathways are independent and distinct. J Biol Chem. 2007; 282:10311–10324. [PubMed: 17284452]
43. Hara MR, Agrawal N, Kim SF, Cascio MB, Fujimuro M, Ozeki Y, Takahashi M, Cheah JH, Tankou SK, Hester LD, Ferris CD, Hayward SD, Snyder SH, Sawa A. S-nitrosylated GAPDH initiates apoptotic cell death by nuclear translocation following Siah1 binding. Nat Cell Biol. 2005; 7:665–674. [PubMed: 15951807]
44. Jones KA, Li DJ, Hui E, Sellmyer MA, Prescher JA. Visualizing cell proximity with genetically encoded bio-luminescent reporters. ACS Chem Biol. 2015; 10:933–938. [PubMed: 25643167]

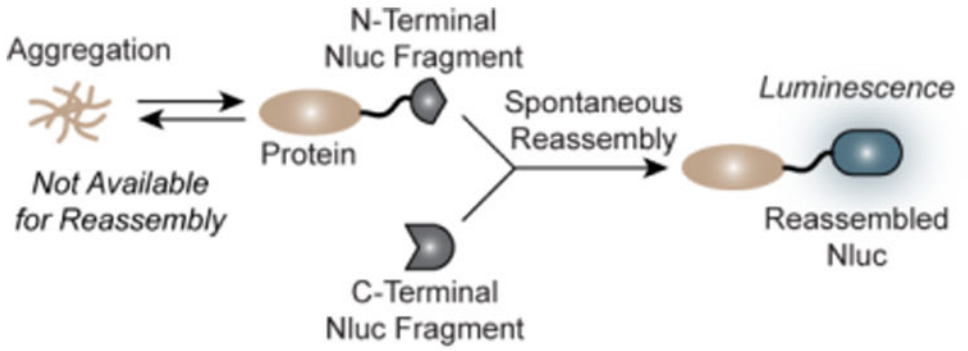

Figure 1.

Schematic of aggregation assay. Fusion of a protein (tan) to the N-terminal Nluc fragment (gray) results in predictable changes in observable luminescence (right) that correlates with the solubility of the appended protein.

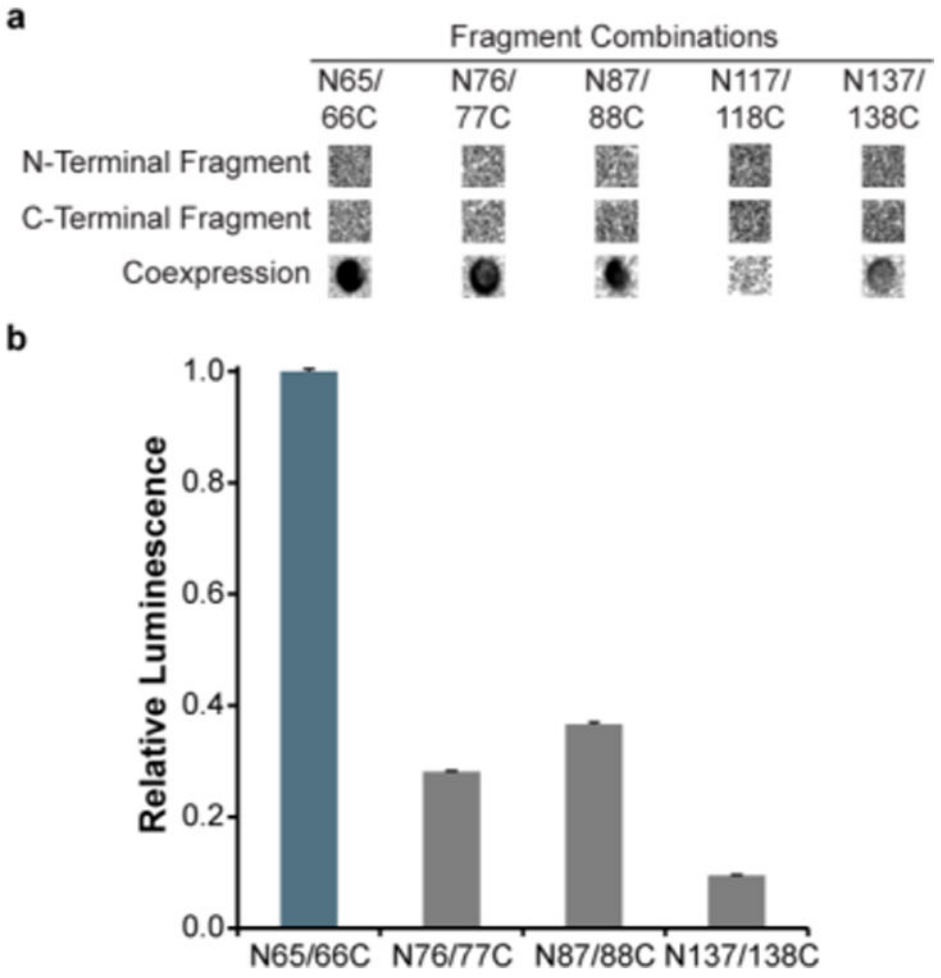

Figure 2.

Spontaneous reassembly of Nluc fragments in bacteria. (a) Luminescence images of bacteria expressing the indicated combinations of Nluc fragments. Full amino acid sequences are given in Table S1. (b) Relative luminescence of bacterial cell suspensions expressing the indicated Nluc fragment combinations. Samples were normalized for cell density. Error bars represent the standard deviation of triplicate experiments.

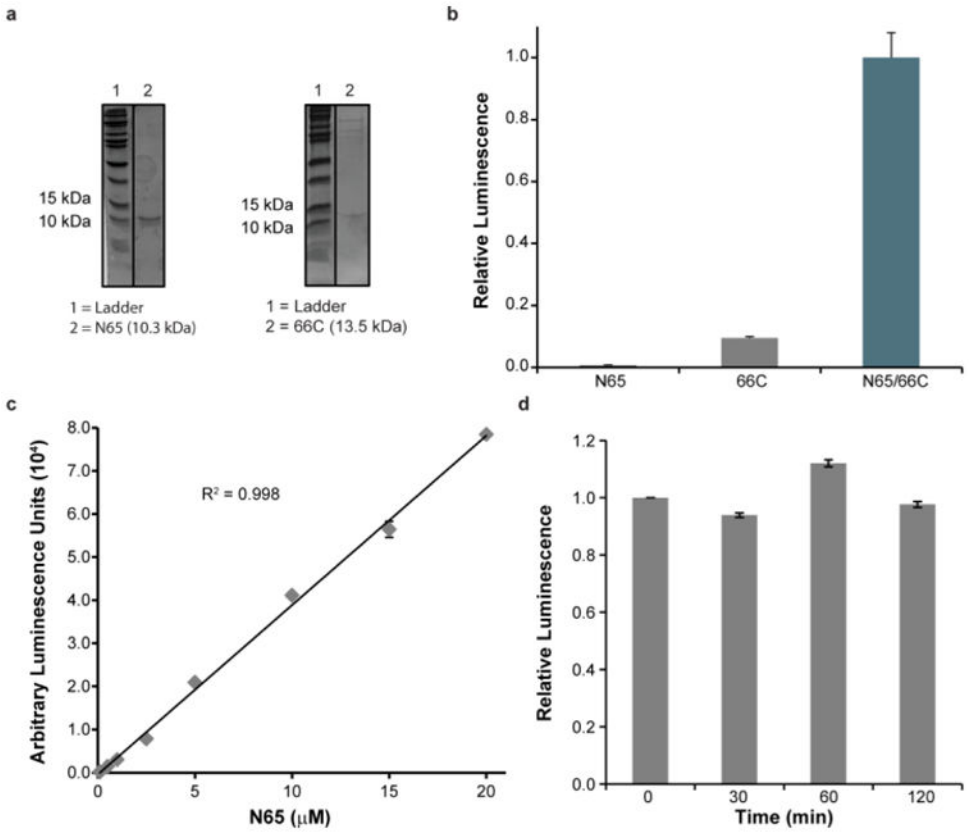

Figure 3. In vitro

characterization of N65 and 66C Nluc fragments. (a) Coomassie stained gels of purified N65 and 66C. (b) Spontaneous reassembly of purified N65 (5 μM) and 66C (50 nM) fragments. Luminescence was measured 50 min after addition of substrate. (c) Luminescence of purified 66C (384 nM) in the presence of increasing concentrations of N65. (d) Luminescence of N65 (250 nM) and 66C (250 nM) fragments assessed at the indicated time after mixing by the addition of coelenterazine. Error bars represent the standard deviation of triplicate experiments.

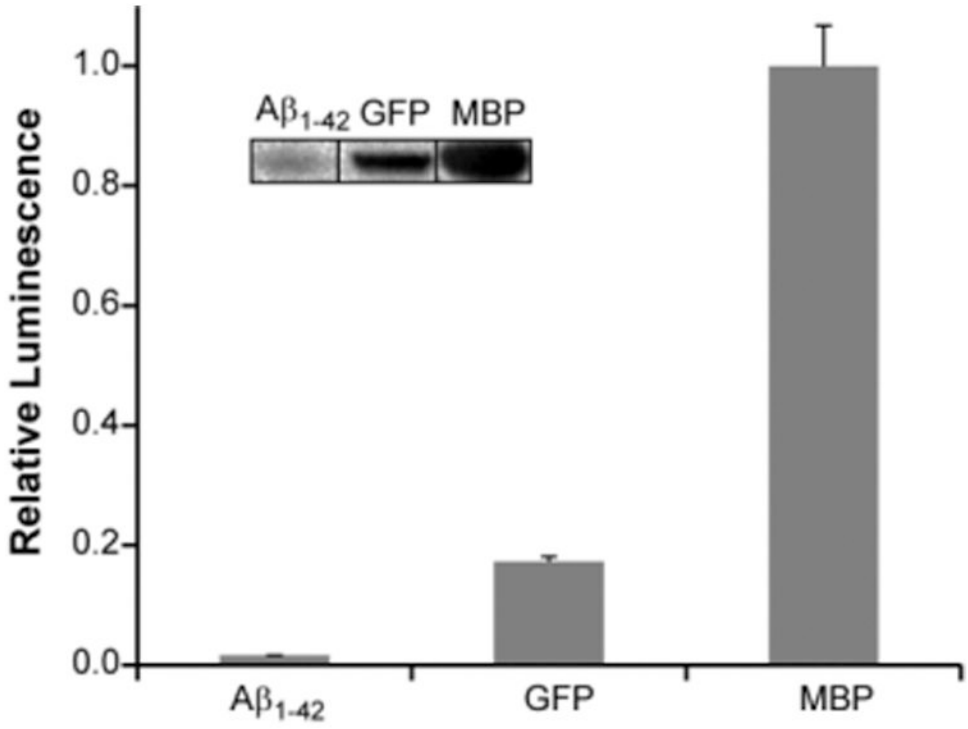

Figure 4.

Effect of soluble N65 concentration on luminescence recovery in bacteria. Luminescence of A$\beta_{1–42}$, GFP, and MBP fusions to N65 assessed in intact bacteria expressing 66C. Observed luminescence correlates with soluble protein as determined by Western blot (inset). Data are normalized for cell density, and error bars represent the standard deviation of triplicate experiments.

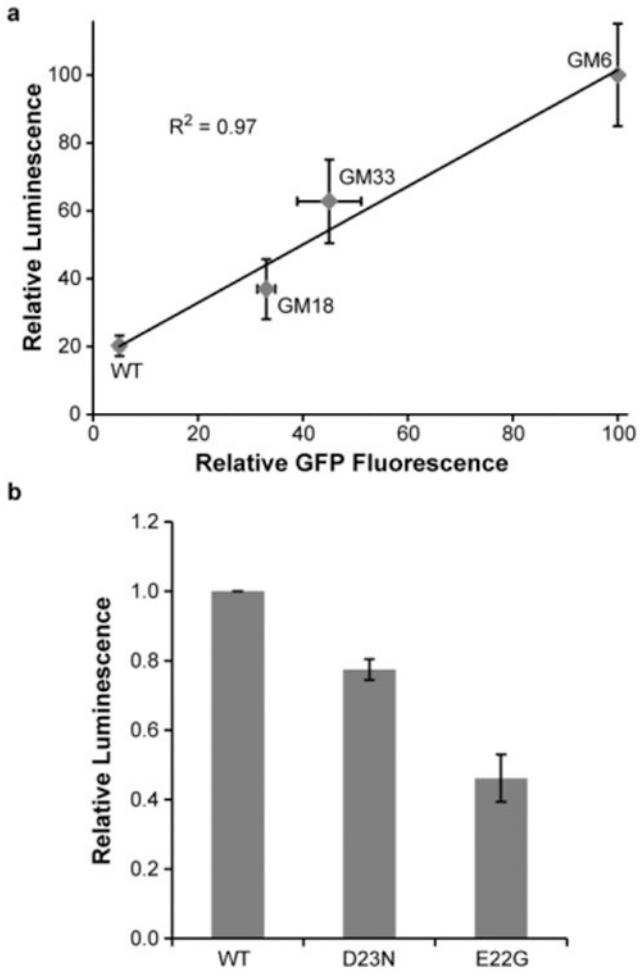

Figure 5.

Monitoring the relative aggregation potential of proteins in bacteria. (a) Bacterial luminescence from the N65/66C system correlates with previously published aggregation potentials for a series of A$\beta_{1–42}$ mutants determined using a GFP-based aggregation assay.[4] A$\beta_{1–42}$ point mutants are GM18 (L34P), GM33 (L34P and A42S), and GM6 (F19S and L34P). WT is wild-type A$\beta_{1–42}$. Error bars for luminescence data represent the standard deviation from triplicate measurements on two separate biological replicates (six total measurements). (b) Luminescence output from bacteria expressing D23N- or E22G-N65 fusions. Error bars represent the standard deviation of triplicate experiments. Data in both panels are normalized for cell density.

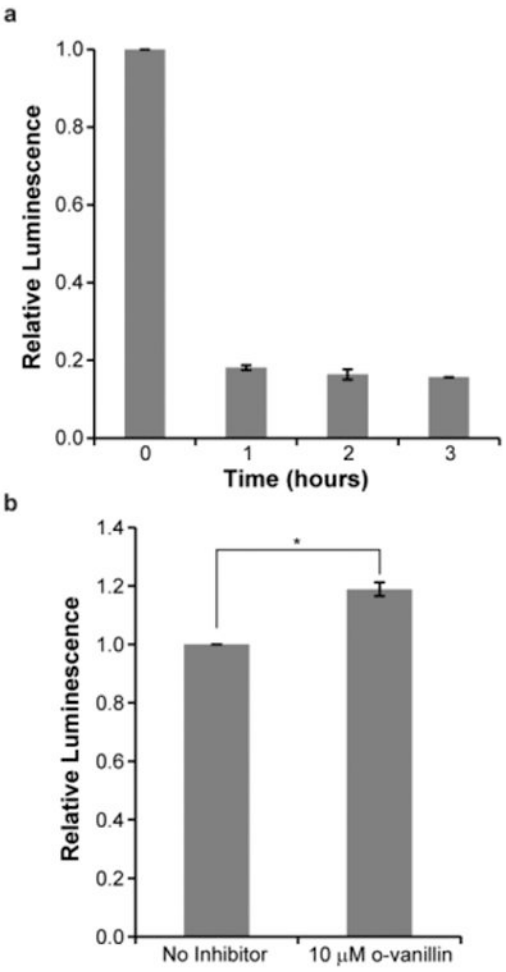

Figure 6.

Monitoring the effect of small molecule inhibitors of protein aggregation. (a) The aggregation of A$\beta_{1–42}$-N65 can be monitored by incubation of A$\beta_{1–42}$-N65 lysate for the indicated time at 37 °C and detection of aggregation by subsequent addition of 66C lysate and coelenterazine. A time-dependent decrease in luminescence is observed. (b) Inhibition of A$\beta_{1–42}$ aggregation is observed in the presence of 10 μM o-vanillin. Lysates containing A$\beta_{1–42}$-N65 were incubated with o-vanillin for 3 h. Aggregation was detected by the addition of lysates containing 66C as well as coelenterazine. * indicates a p value of 0.001. Error bars represent the standard deviation of triplicate experiments.

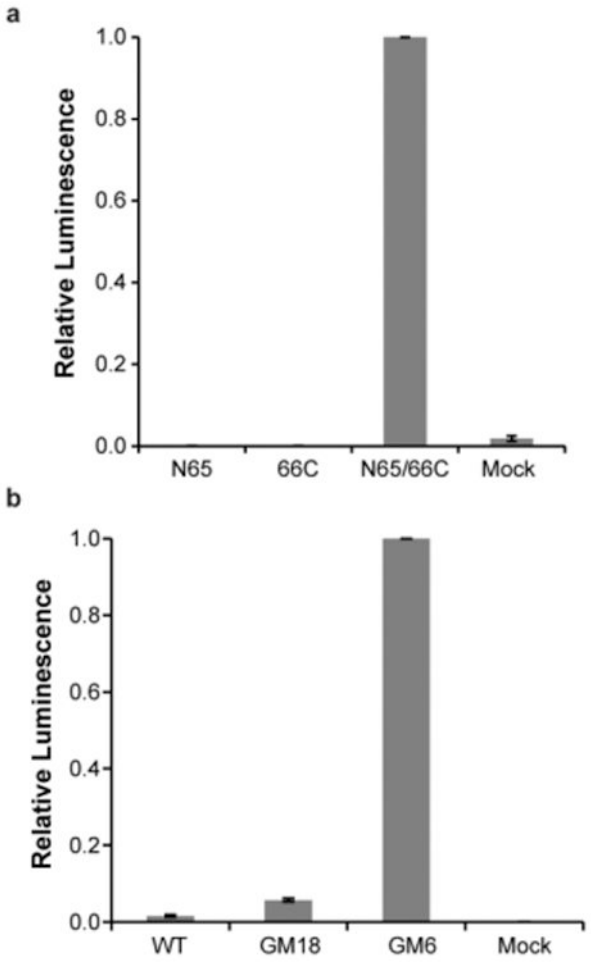

Figure 7.

Aggregation assays can be ported into mammalian cells. (a) Luminescence of NIH-3T3 cells transfected with plasmids encoding the indicated Nluc fragments. Luminescence is only observed when both N65 and 66C are present. (b) Luminescence output resulting from expression of A$\beta_{1–42}$ mutants fused to N65 correlates with the known aggregation potential of these proteins (see Figure 5a). Error bars represent the standard deviation of triplicate experiments.